Vol 17 No 4, April 2008
1674-1056/2008/17(04)/1377-06

Chinese Physics B

© 2008 Chin. Phys. Soc.
and IOP Publishing Ltd

First-principles investigations on elastic and thermodynamic properties of zinc-blende structure BeS*

Chang Jing(常 景)[a], Chen Xiang-Rong(陈向荣)[a)b)†]
Zhang Wei(张 伟)[a], and Zhu Jun(朱 俊)[a]

[a] *College of Physical Science and Technology, Sichuan University, Chengdu* 610064, *China*

[b] *International Centre for Materials Physics, Chinese Academy of Sciences, Shenyang* 110016, *China*

(Received 24 August 2007; revised manuscript received 8 October 2007)

In this paper the elastic and thermodynamic properties of the cubic zinc-blende structure BeS at different pressures and temperatures are investigated by using *ab initio* plane-wave pseudopotential density functional theory method within the generalized gradient approximation (GGA). The calculated results are in excellent agreement with the available experimental data and other theoretical results. It is found that the zinc-blende structure BeS should be unstable above 60GPa. The thermodynamic properties of the zinc-blende structure BeS are predicted by using the quasi-harmonic Debye model. The pressure-volume-temperature ($P-V-T$) relationship, the variations of the thermal expansion coefficient α and the heat capacity C_V with pressure P and temperature T, as well as the Grüneisen parameter-pressure-temperature ($\gamma - P - T$) relationship are obtained systematically in the ranges of 0–90GPa and 0–2000K.

Keywords: density functional theory, elastic constants, thermodynamic properties, Grüneisen parameter, BeS

PACC: 7115M, 6220D, 6740K, 7470F

1. Introduction

In view of increasing need of potentially good semiconductors for various electrical and optical devices, the II-VI semiconductors AX (A = Be, Mg, Ca, Ba; X = O, S, Se, Te) compounds have been extensively studied in recent years.[1−5] They have been the subject of vast amount of theoretical and experimental work during the past decades, motivated in part by their technological usefulness and their remarkable and interesting physical properties. Therefore, beryllium chalcogenides (BeS, BeSe and BeTe) are also drawn great attentions.[1−5] Beryllium chalcogenides have a much higher degree of covalent binding and are characterized by their small ionic radius ratio in comparison with other wide-gap II-VI semiconductors. They can be grown on various substrates by molecular beam epitaxy (MBE).[6]

At present, there exist many investigations on the electronic band structure and density of states of these BeX compounds.[1−5] The high pressure structural phase transformation from the zinc-blende (ZB) structure to the nickel-arsenide (NiAs) structure has also been reported to occur at 51 GPa with a volume change of 11%.[7] However, there are few literatures reporting on the elastic and thermodynamic properties of BeX at different pressures and temperatures.

In this work, we give a detailed description for the elastic and thermodynamic properties of the cubic ZB structure BeS at different pressures and temperatures through the Cambridge Serial Total Energy Package (CASTEP) program[8,9] and the quasi-harmonic Debye model.[10] The structure and elastic constants obtained are in agreement with the experimental data and other theoretical results. In Sec.2, we make a brief review of the theoretical method. The results and some discussions are presented in Sec.3.

2. Theoretical method

2.1. Total energy electronic structure calculation

In our electronic structure calculations, we adopt the non-local ultrasoft pseudopotential introduced by

*Project supported by the National Natural Science Foundation of China (Grant No 10576020) and the NSAF (Grant No 10776022).
†Corresponding author. E-mail: xrchen@126.com

Vanderbilt[11] for the interactions of the electrons with the ion cores, together with the generalized gradient approximation (GGA) for exchange-correlation functional in the scheme of Perdew–Burke–Ernzerhof (PBE).[12] The electronic wave functions are expanded in a plane wave basis set with energy cut-off of 340 eV. Pseudo-atom calculations are performed for S $3s^2 3p^4$ and Be $2s^2$. For the Brillouin-zone k-point sampling, we use the Monkhorst–Pack mesh with 8×8×8 k-points, where the self-consistent convergence of the total energy is 5.0×10^{-8} eV/Atom. These parameters are sufficient in leading to well converged total energy, geometrical configurations and elastic stiffness coefficients. All total energy electronic structure calculations are implemented through the CASTEP code.[8,9]

2.2. Elastic properties

The elastic stiffness tensor relates to the stress tensor and the strain tensor by Hooke's law. Since the stress and strain tensors are symmetric, the most general elastic stiffness tensor has only 21 non-zero independent components. For a cubic crystal, they are reduced to three components, i.e. C_{11}, C_{12}, and C_{44}. These elastic stiffness coefficients (namely the elastic constants) can be determined by computing the stress generated by forcing a small strain to an optimized unit cell.[13,14] Moreover, the adiabatic bulk $B_{\rm S}$ and the shear modulus$G$ are given by[15]

$$B_{\rm S} = (C_{11} + 2C_{12})/3, \tag{1}$$

$$G = (G_{\rm V} + G_{\rm R})/2, \tag{2}$$

where C=$(C_{11} - C_{12})/2$, $G_{\rm V}$= $(2C$+3$C_{44})/5$, $G_{\rm R}$ = 15*$(6/C$+9$/C_{44})^{-1}$, $G_{\rm V}$ is the Voigt shear modulus and $G_{\rm R}$ is the Reuss shear modulus. For cubic crystals, mechanical stability of crystals is judged by the following conditions:[16]

$$\tilde{C}_{44} > 0, \quad \tilde{C}_{11} > \left|\tilde{C}_{12}\right|, \quad \tilde{C}_{11} + 2\tilde{C}_{12} > 0, \tag{3}$$

where $\tilde{C}_{\alpha\alpha} = C_{\alpha\alpha} - P(\alpha$=1,4), $\tilde{C}_{12} = C_{12} + P$.

An important parameter is the internal strain parameter ξ introduced by Kleinman,[17] which describes the relative positions of the cation and anion sublattices under volume, conserving strain distortions, for which positions are not fixed by symmetry. The parameter ξ can be obtained from[18,19]

$$\xi = \frac{C_{11} + 8C_{12}}{7C_{11} + 2C_{12}}. \tag{4}$$

2.3. Thermodynamic properties

To investigate the thermodynamic properties of BeS, we here apply the quasi-harmonic Debye model.[10] In the quasi-harmonic Debye model, the non-equilibrium Gibbs function $G*(V;P,T)$ is taken in the form of

$$G*(V;P,T) = E(V) + PV + A_{\rm Vib}(\Theta(V);T), \tag{5}$$

where $E(V)$ is the total energy, PV corresponds to the constant hydrostatic pressure condition, Θ (V) is the Debye temperature, and the vibrational contribution $A_{\rm Vib}$ can be written as[20,21]

$$A_{\rm Vib}(\Theta;T) = nk_{\rm B}T\left[\frac{9}{8}\frac{\Theta}{T} + 3\ln(1-{\rm e}^{-\Theta/T}) - D(\Theta/T)\right], \tag{6}$$

where $D(\Theta/T)$ represents the Debye integral, n is the number of atoms per formula unit. For an isotropic solid, Θ is expressed by[20]

$$\Theta_{\rm D} = \frac{\hbar}{k_{\rm B}}\left[6\pi^2 V^{1/2} n\right]^{1/3} f(\sigma)\sqrt{\frac{B_{\rm S}}{M}}, \tag{7}$$

where M is the molecular mass per unit cell, $B_{\rm S}$ is the adiabatic bulk modulus, which can be approximated by the static compressibility[22]

$$B_{\rm S} \cong B(V) = V\left\{\frac{{\rm d}^2 E(V)}{{\rm d}V^2}\right\}, \tag{8}$$

$f(\sigma)$ is given by Ref.[22],

$$f(\sigma) = \left\{3\left[2\left(\frac{2(1+\sigma)}{3(1-2\sigma)}\right)^{3/2} + \left(\frac{1+\sigma}{3(1-\sigma)}\right)^{3/2}\right]^{-1}\right\}^{1/3}, \tag{9}$$

the Poisson ratio σ is taken as 0.25.[23] Therefore, the non-equilibrium Gibbs function $G^*(V;P,T)$ as a function of $(V;P,T)$ can be minimized with respect to volume V,

$$\left(\frac{\partial G^*(V;P,T)}{\partial V}\right)_{P,T} = 0. \tag{10}$$

By solving Eq.(10), one can get the thermal equation of state (EOS) V $(P,\ T)$. The isothermal bulk modulus $B_{\rm T}$, the heat capacity C_V, and the thermal expansion coefficient α are given by[10]

$$B_{\rm T}(P,T) = V\left(\frac{\partial^2 G^*(V;P,T)}{\partial V^2}\right)_{P,T}, \tag{11}$$

$$C_V = 3nk_{\rm B}\left[4D(\Theta/T) - \frac{3\Theta/T}{{\rm e}^{\Theta/T}-1}\right], \tag{12}$$

$$\alpha = \frac{\gamma C_V}{B_{\rm T} V}, \tag{13}$$

where γ is the Grüneisen parameter, which is defined as

$$\gamma = -\frac{\mathrm{d}\ln\Theta(V)}{\mathrm{d}\ln V}. \tag{14}$$

Applying these methods described above, we have successfully investigated the thermodynamic properties of some materials.[24−27]

3. Results and discussion

Firstly, we set a series of different values of lattice constant a to calculate the total energy E and the corresponding primitive cell volume V for the ZB structure BeS at P=0 GPa and T=0K, and then fit the calculated $E-V$ data to the natural strain EOS[28]

$$P = 2B_0\left(\frac{V_0}{V}\right)f_N\left[1+\frac{3}{2}\left(B'-2\right)f_N+\frac{3}{2}\left(1+B^0B''+\left(B'-2\right)+\left(B'-2\right)^2\right)f_N^2\right], \tag{15}$$

where $f_N = \ln(l/l_0)$, which may be written as $f_N = \ln(V/V_0)/3$ for hydrostatic compression. The obtained lattice constant a, bulk modulus B_0 and its pressure derivative B_0', as well as the elastic constants at P=0 GPa and T=0 K are presented in Table 1, together with the available experimental values[29] and other theoretical results.[1,30−34] The agreement among them is good.

The pressure and temperature dependences of the relative volume V/V_0 of the ZB structure BeS are illustrated in Fig.1. It is seen that, as the pressure P increases, the relative volume V/V_0 decreases at a given temperature, and the relative volume V/V_0 of higher temperature is less than that of lower temperature at the same pressure. On the other hand, the volume V decreases with the elevated pressure P, and increases with the elevated temperature T. This effect of increasing pressure on BeS is just the same as decreasing temperature of BeS.

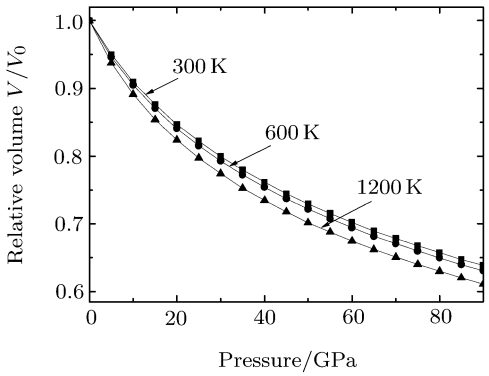


Fig.1. Relative volume versus pressure of the ZB structure BeS at 300, 600 and 1200 K, respectively.

Table 1. Lattice constant a, bulk modulus B_0 and its pressure derivative B_0', adiabatic bulk B_S, together with the experimental data and other theoretical results for the ZB structure BeS at 0 GPa and 0 K.

	$a/10^{-1}$nm	B_0/GPa	B_0'/GPa	C_{11}/GPa	C_{12}/GPa	C_{44}/GPa	ξ	B_S/GPa
Present	4.861	96.03	3.5	155.14	61.45	81.66	0.53	92.7
Expt.[28]	4.87	105	3.5					
WIEN2k[1]	4.80	100.8	3.63	167	68	105	0.42	
FP-LAPW[30]	4.803	103.7	3.49	143.1	84	91.1		
TB-LMTO[31]	4.839	102.8						
TB-LMTO[32]	4.806	110.7	3.671	140.32	95.92	23.89		
PP[33]	4.745	116		184	75	99	0.544	
PP[34]	4.745	116	3.22					

In Table 2, we present the pressure dependences of the elastic constants C_{ij}, the aggregate elastic modulus B, G for the ZB structure BeS at 0–90 GPa. Unfortunately, no experimental and theoretical data of elastic constants are available for our comparison. In Fig.2, we illustrated the variation of elastic constants and bulk modulus and shear wave modulus of BeS with respect to the variation of pressure. It is shown from Table 2 that the elastic constants C_{11}, C_{12}, C_{44}, bulk modulus B and shear wave modulus C_S linearly increase monotonously when pressure is enhanced. Moreover, C_{44} and C_S increase very slowly

with the elevated pressure. The elastic constants are not content with $\tilde{C}_{11} > \left|\tilde{C}_{12}\right|$ when the applied pressure is above 60 GPa, indicating that the ZB structure BeS should be unstable above 60 GPa. Narayana *et al* reported that the high pressure structural phase transformation from the ZB structure to the NiAs structure BeS occurs at 51 GPa.[7] Our results are consistent with theirs. On the other hand, for the shear waves of the ZB structure BeS, the wave polarized perpendicular to the basal plane (S1) and the one polarized in the basal plane (S2) have the anisotropies

$$\Delta_{\mathrm{S1}} = \frac{1}{\Delta_{\mathrm{S2}}} = \frac{C_{11} - C_{12}}{2C_{44}}. \tag{16}$$

In Table 2, we also list the calculated Δ_{S1}. It is noted that, Δ_{S1} generally descends as pressure increases from 0 to 90 GPa except at 60 GPa (due to the fact that the ZB-NiAs structural phase transformation occurs for BeS). As pressure increases, the anisotropy will strengthen.

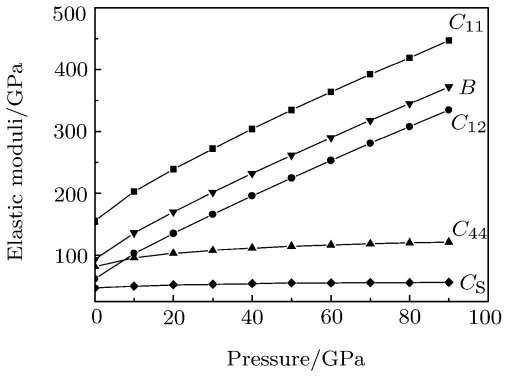


Fig.2. Calculated pressure dependence of C_{ij}, C_{S} and B for the ZB structure BeS.

Table 2. Calculated lattice parameters a, elastic constants C_{ij} and aggregate elastic moduli B, B_0', G, and the shear wave modulus C_{S} of the ZB structure BeS under pressure at zero temperature.

P/GPa	$a/10^{-1}$nm	C_{11}/GPa	C_{12}/GPa	C_{44}/GPa	B/GPa	B_0'/GPa	G/GPa	C_{S}/GPa	Δ_{S1}
0	4.86	155.137	61.500	81.659	92.71	3.81	65.33	46.82	0.573
10	4.686	202.857	102.730	95.669	136.11	3.39	73.78	50.06	0.523
20	4.581	238.831	135.162	103.004	169.72	3.17	78.20	51.83	0.503
30	4.497	271.980	166.007	107.805	201.33	3.03	81.07	52.99	0.492
40	4.426	303.987	195.875	111.609	231.91	2.93	83.43	54.06	0.484
50	4.365	334.600	224.825	114.574	261.42	2.85	85.27	54.89	0.471
60	4.311	363.708	252.964	116.461	289.88	2.78	86.42	55.37	0.475
70	4.262	392.216	280.761	118.466	317.91	2.73	87.53	55.73	0.470
80	4.219	419.300	307.847	120.101	344.99	2.67	88.23	55.73	0.464
90	4.179	447.019	334.620	121.374	372.08	2.62	89.11	56.20	0.463

In Table 3, we list the heat capacity and the Debye temperature at different temperatures (300 K, 600 K, 1200 K) and different pressures (0 GPa, 10 GPa, 20 GPa, 30 GPa, 40 GPa, 50 GPa, 60 GPa). It is found that, when the applied pressure is from 0 GPa to 60 GPa, the heat capacity decreases by 29.05%, 9.38%, 2.59%, 1.51%, 1.22%, and the Debye temperature increases by 66.41%, 69.98%, 79.99% at 300 K, 600 K, and 1200 K, respectively. As the pressure increases, the heat capacity decreases more quickly at low temperature than at high temperature. The Debye temperatures Θ increase more quickly at high temperature than at low temperature.

Table 3. Heat capacity C_V, Debye temperature Θ, and Grüneisen constant γ of the ZB structure BeS at temperatures T and pressures P.

T/K	P/GPa	0	10	20	30	40	50	60
300	C_V/J·mol^{-1}·K^{-1}	40.068	37.230	34.930	32.990	31.296	29.785	28.428
	Θ/K	643.18	749.22	832.64	902.65	964.12	1019.63	1070.34
	γ	1.703	1.525	1.437	1.377	1.328	1.285	1.246
600	C_V/J·mol^{-1}·K^{-1}	47.271	46.314	45.493	44.755	44.073	43.436	42.837
	Θ/K	626.39	737.31	822.88	894.48	957.21	1013.51	1064.72
	γ	1.743	1.540	1.446	1.384	1.334	1.290	1.251
1200	C_V/J·mol^{-1}·K^{-1}	49.302	49.024	48.794	48.585	48.388	48.199	48.026
	Θ/K	583.77	710.14	800.59	875.39	940.41	999.34	1050.74
	γ	1.862	1.578	1.468	1.400	1.347	1.301	1.261

Figure 3 shows the predicted $P-\alpha$ and $T-\alpha$ relationship curves for the ZB structure BeS. It is shown that, for a given temperature, α decreases drastically with the increase of pressure. When the pressure is above 60 GPa, the thermal expansion coefficient α of 1200 K is just a little larger than that of 600 K. While for a given pressure, α increases rapidly with temperature especially at low temperature at zero pressure, However, when $T > 500$ K and $P > 30$ GPa gradually approaches a linear increase at high temperatures, which means that the temperature dependence of α is very small at high pressure and high temperature.

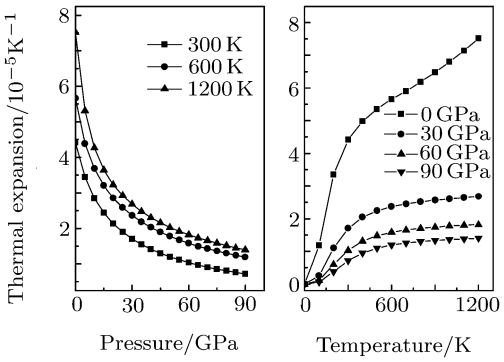


Fig.3. Thermal expansion versus pressure and temperature for the ZB structure BeS.

Grüneisen constant γ, which describes the anharmonic effects in the vibrating lattice, can correctly predict the anharmonic properties of a material, such as the thermal expansion coefficient and the temperature dependence of phonon frequencies and linewidths. Moruzzi *et al* [35] reviewed that the Grüneisen parameter is dominated by lower-frequency transverse modes at low temperature. The Slater's expression for γ assumes that equal excitation of all modes is effectively at high-temperature. In Table 3, we also list the obtained Grüneisen constant γ. It is noted that the Grüneisen constant γ decreases with increasing pressure at constant temperature, and increases with increasing temperature at constant pressure.

In summary, the elastic and thermodynamic properties of the cubic zinc-blende structure BeS at different pressures and temperatures are investigated by using *ab initio* plane-wave pseudopotential density functional theory method within the generalized gradient approximation (GGA). The calculated results are in excellent agreement with the available experimental data and other theoretical results. It is found that the ZB structure BeS should be unstable above 60 GPa. The thermodynamic properties of the zinc-blende structure BeS are predicted by using the quasi-harmonic Debye model. The pressure-volume-temperature ($P-V-T$) relationship, the variations of the thermal expansion coefficient α and the heat capacity C_V with pressure P and temperature T, as well as the Grüneisen parameter-pressure-temperature ($\gamma-P-T$) relationships are obtained systematically in the ranges of 0–90 GPa and 0–2000 K.

References

[1] Khenata R, Bouhemadou A, Hichour M, Baltache H, Rached D and Rerat M 2006 *Solid-State Electronics* **50** 1382

[2] Yadav P S, Yadav R K, Agrawal S and Agrawal B K 2007 *Physica* E **36** 79

[3] Benosman N, Amrane N, Mecabih S and Aourag H 2001 *Physica* B **304** 214

[4] Heciri D, Beldi L, Drablia S, Meradji H, Derradji N E, Belkhir H and Bouhafs B 2007 *Comput. Mater. Sci.* **38** 609

[5] Rached D, Rabah M, Benkhettou N, Khenata R, Soudini B, Al-Douri Y and Baltache H 2006 *Comput. Mater. Sci.* **37** 292

[6] Waag A, Fischer F, Lugauer H J, Litz T H, Laubender J, Lunz U, Zehnder U, Ossau W, Gerhardt T, Moller M and Landwehr G 1996 *J. Appl. Phys.* **80** 792

[7] Narayana C, Nesamony V J and Ruoff A L 1997 *Phys. Rev.* B **56** 22

[8] Payne M C, Teter M P, Allen D C, Arias T A and Joannopoulos J D 1992 *Rev. Mod. Phys.* **64** 1045

[9] Milan V, Winker B, White J. A , Packard C J, Payne M C, Akhmatskaya E V and Nobes R H 2002 *Int. J. Quantum Chem.* **77** 85

[10] Blanco M A, Francisco E and Luana V 2004 *Comput. Phys. Commun.* **158** 57

[11] Vanderbilt D 1990 *Phys. Rev.* B **41** 7892

[12] Perdew J P, Burke K and Ernzerhof M 1996 *Phys. Rev. Lett.* **77** 3865

[13] Karki B B, Stixrude L, Clark S J, Warren M C, Ackl and G J and Crain J 1997 *Am. Miner.* **82** 51

[14] Wentzcovitch R M, Ross N L and Price G D 1995 *Phys. Earth Planet. Inter.* **90** 101

[15] Zha C S, Mao H K and Hemley R J 2000 *Proc. Natl. Acad. Sci. USA.* **97** 13494

[16] Sinko G V and Smirnow N A 2002 *J. Phys.: Condens. Matter* **14** 6989

[17] Kleinman L 1962 *Phys. Rev.* **128** 2614

[18] Kanoun M B, Merad A E, Cibert J, Aourag H and Merad G 2004 *J. Alloys Compnd.* **366** 86

[19] Merad A E, Aourag H, Khalifa B, Mathieu C and Merad G 2001 *Superlatt. Microstruct.* **30** 241

[20] Blanco M A, Martín Pendás A, Francisco E, Recio J M and Franco R 1996 *J. Mol. Struct.* (*Theochem.*) **368** 245

[21] Flórez M, Recio J M, Francisco E, Blanco M A and Pendás A M 2002 *Phys. Rev.* B **66** 144112
[22] Francisco E, Blanco M A and Sanjurjo G 2001 *Phys. Rev.* B **63** 094107
[23] Poiier J P 1991 *Introduction to the Physics of the Earth's Interior* (Cambridge: Cambridge University Press) p312
[24] Li X F, Chen X R, Meng C M and Ji G F 2006 *Solid State Commun.* **139** 197
[25] Hao Y J, Cheng Y, Wang Y J and Chen X R 2007 *Chin. Phys.* **16** 217
[26] Zhou X L, Liu K, Chen X R and Zhu J 2006 *Chin. Phys.* **15** 3014
[27] Cheng Y, Lu L Y, Jia O H and Chen X R 2008 *Chin. Phys.* **17** (in Press)
[28] Poirier J P and Tarantola A 1998 *Phys. Earth Planet Int.* **109** 1
[29] Narayana C, Nesamony V J and Ruoff A L 1997 *Phys. Rev.* B **56** 14338
[30] El Haj, Hassan F and Akbarzadeh H 2006 *Comput. Mater. Sci.* **35** 423
[31] Kalpana G, Pari G, Mookerjee A and Bhattacharyya A K 1998 *Int. J. Mod. Phys.* B **12** 1975
[32] Rached D, Rabah M, Benkhettou N, Khenata R, Soudini B, Al-Douri Y and Baltache H 2006 *Comput. Mater. Sci.* **37** 292
[33] Gonzalez-Diaz M, Rodrigune-Hernandez P and Munoz A 1997 *Phys. Rev.* B **55** 14043
[34] Munoz A, Rodriguez-Hernandez P and Mujica A 1996 *Phys. Rev.* B **54** 11861
[35] Moruzzi V L, Janak J F and Schwarz K 1998 *Phys. Rev.* B **37** 790